Article:

Henthorn, S. orcid.org/0000-0003-1913-9283, Ford, K.L. orcid.org/0000-0002-1080-6193 and O'Farrell, T. orcid.org/0000-0002-7870-4097 (2022) A system-level performance evaluation of a reconfigurable filtenna in the presence of in- and out-of-band blockers. IET Communications, 16 (20). pp. 2492-2500. ISSN 1751-8628

https://doi.org/10.1049/cmu2.12504

Received: 23 June 2022 | Revised: 2 September 2022 | Accepted: 15 September 2022

DOI: 10.1049/cmu2.12504

IET Communications

The Institution of Engineering and Technology WILEY

ORIGINAL RESEARCH

A system-level performance evaluation of a reconfigurable filtenna in the presence of in- and out-of-band blockers

Stephen Henthorn | Kenneth Lee Ford | Timothy O'Farrell

Department of Electronic and Electrical Engineering, University of Sheffield, Sheffield, UK

Correspondence
Stephen Henthorn, Department of Electronic and Electrical Engineering, University of Sheffield, Sheffield, UK.
Email: s.henthorn@sheffield.ac.uk

Funding information
Engineering and Physical Sciences Research Council, Grant/Award Numbers: EP/M013723/1, EP/S008101/1

Abstract

Direct RF sampling has been suggested as a solution for receivers that are flexible in frequency and across standards, while utilising only a single radio frequency front-end. However there are concerns about their robustness in the presence of out-of-band and in-band blockers. Tunable filtennas offer a solution to this, incorporating filtering into the antenna space while providing rejection of unwanted signals. This paper presents a filtenna containing reconfigurable frequency selective surfaces to provide tunable filtering between 1.44 and 1.95 GHz. The filtenna is characterised as an antenna and a filter, showing minimum 18 dB rejection across the principle beamwidths. It is then implemented in a direct RF sampling receiver and is shown to provide sufficient rejection of blockers to cause no degradation in the received error vector magnitude (EVM) and block error rate (BLER) of LTE signals when subject to 5G NR-compliant blocking signals. The in-band blocker performance is also characterised, showing at most 3 dB degradation in EVM and BLER.

1 | INTRODUCTION

As the number of wireless communications standards increases, the requirement of base stations and access points to have multiple radio receivers increases the space and so expenditure required for each site. Direct sampling software defined radio (SDR) has been suggested as a solution to this problem, by using a high-speed and bandwidth analogue to digital converter (ADC) to sample at radio frequency (RF), then allocating digital resources dynamically to perform downconversion and baseband processing, allowing reconfigurable multi-standard operation [1]. However, there is still a requirement for a RF front-end capable of receiving, filtering and amplifying RF signals in order to select desired signals and mitigate the effect of blocking signals. Typically this involves at least one antenna, band filter and low noise amplifier (LNA), possibly one per band in tuneable or multi-band receivers. Several approaches to designing these front-ends have been suggested to reduce the footprint of the RF front-end. One such uses a reconfigurable narrowband antenna in combination with a tuneable notch filter targeted at removing the duplex transmit frequency [2]. Other approaches use tuneable multi-band antennas combined with a wideband LNA and static filters to provide multi-band performance [3, 4]. However, these approaches still utilise independent antennas, filters and amplifiers.

The filtering antenna, or filtenna, has been suggested as a way to combine the antenna and band filtering into a single space. An early and influential work used a substrate-integrated waveguide-inspired frequency selective surface (FSS) inside a horn antenna to reject signals outside its 1.5-GHz bandwidth [5]. Research focus has since then mainly been for user equipment (UE) applications, such as adding notch filters to the feedline of ultrawideband antennas [6]. The potential applications of reconfigurable versions of filtennas were noted, and their use in SDR and cognitive radio (CR) suggested [7]. Various approaches to reconfigurable filtennas include integrating PIN diodes into a slot antenna to switch between two bands [8], and incorporating reconfigurable bandpass filters in the feedline of a wideband patch antenna. This latter technique has been applied with both PIN diodes in order to switch between different bands [7], and with varactor diodes for continuously tuneable filtering [9], while others have used both, with tuning diodes at low frequency for narrowband responses, but the ability to switch to a wideband higher frequency response [10].

While one of the key purposes of filtennas is to prevent unwanted signals causing degradation of receiver performance, system-level investigations of filtennas are rare in the literature. One example uses a static filtenna to remove amplifier non-linearities in a transmitter [11]. The filtenna is a static microstrip antenna and is implemented in a wireless pressure monitoring system, but the performance of the filtenna in receive mode is not evaluated. The only other example the authors could find in the literature investigating the performance of filtennas in communications systems utilises a tuneable filtenna with two modes: a continuously tuneable mode from 430 to 650 MHz, and a static broadband mode for 1 to 5 GHz [12]. The tuneable region has calculated efficiencies of between 22% and 30% giving gains between −14 and −6 dBi. It is integrated with a commercial-off-the-shelf SDR receiver, and the bit error rate (BER) of a QPSK modulated signal is measured, showing the BER can reduce below 0.1% at signal-to-noise ratios (SNRs) of over 9 dB in the tuneable region. It is not clear whether the receiver utilises conventional analogue downconversion, or direct RF sampling capabilities, and the receiver performance is not investigated in the presence of any unwanted signals.

The key contribution of this paper is the evaluation of a tunable filtenna-based direct RF sampling receiver in the presence of unwanted blocking signals. The filtenna is introduced, its key characteristics are measured, and then it is integrated into a direct RF sampling SDR receiver architecture. Using LTE signals, the receiver performance is characterised both on its own and with out-of-band (OOB) blocking and adjacent channel selectivity (ACS) performance. The strength of the blockers is determined using 5G NR over-the-air (OTA) standard tests. The filtenna used in this proof-of-principle demonstration was previously developed for direct antenna modulation and contains a multi-layer tunable FSS [13]. New measurements exploring its performance as a reconfigurable filtenna in a tunable direct RF sampling receiver are presented, which is an advance over the static FSS in [5] and the switchable band-stop FSS design in [14].

The paper proceeds as follows: in Section 2, the overall vision of a direct RF sampling receiver architecture consisting only of a tunable filtenna, an amplification stage, an ADC and software processing is introduced. Next, the FSS-based filtenna is discussed in Section 3 and its performance measured as both an antenna and as a filter. The filtenna is then implemented in a hardware-in-the-loop (HWIL) OTA testbed in Section 4, and the emulated receiver's performance is measured in the presence of in-band and out-of-band blockers. Finally, conclusions are drawn in Section 5.

2 | FILTENNA-BASED SDR RECEIVER ARCHITECTURE

The filtenna-based direct sampling receiver architecture is shown in Figure 1. The RF front-end consists only of a reconfigurable filtenna and a wideband LNA. This combination means the filtenna must tune over the frequency region of interest, providing good signal reception inside the desired bandwidth

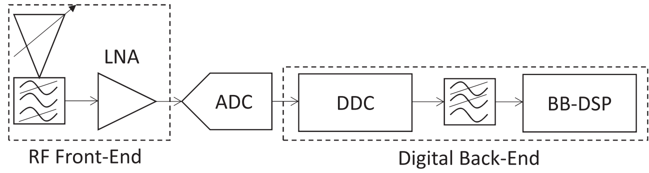

FIGURE 1 Tunable low-complexity receiver architecture using a filtenna

and good rejection outside of it, while the LNA should amplify across the entire frequency region. The filtered and amplified RF is then sampled by an ADC with an analogue bandwidth of at least the maximum frequency of interest, at a sample rate of over twice the maximum frequency of interest. While subsampling techniques could be used to reduce the required sample rate [15], using Nyquist sampling here ensures that the RF signal is recreated accurately in the digital domain with minimal digital noise folding effects. Note some automatic gain control (AGC) may be needed in conjunction with the ADC to ensure the signal fills its dynamic range, though this may be implemented within the LNA.

Resources for the digital back-end can then be assigned dynamically. The digital downconverter (DDC) mixes the signal from the RF carrier frequency to baseband, and a digital low-pass filter (LPF) is applied. Both the frequency of the DDC digitally controlled oscillator (DCO) and the bandwidth of the LPF can be altered easily, allowing the tunable and variable bandwidth operation. Finally, baseband processing is also software controlled, allowing multiple standards to be used in the same resource.

As such, the proposed filtenna-based direct RF sampling receiver architecture utilises a minimal RF front-end to provide good selection of the desired signal from over a broad range of frequencies, while programmable digital capability allows fully flexible downconversion and baseband processing of those signals.

3 | RECONFIGURABLE FILTENNA

The filtenna used in this work was first developed and evaluated as a modulating antenna [13], and is shown schematically in Figure 2 and photographed in Figure 3. It contains a four-layer reconfigurable bandpass FSS (Figure 2b), which enables the filtenna to act as a tunable filter. Each layer of the FSS consist of a 5x5 grid of unit cells each embedded with varactor diodes to allow tuning of the filter response. The substrate is FR4, and on the rear of each FSS is a network of bias lines to enable connection of the bias voltage to each FSS patch. The multi-layer FSS is integrated into a cavity-backed waveguide with a monopole feed. In order to provide bias to all the FSS, 1-mm diameter apertures were fabricated in the waveguide near each FSS and twisted pairs of wires inserted. 10 kΩ resistors were connected to the biasing wires outside the waveguide to act as RF chokes in order to minimise RF currents that might couple into the bias wires and leak into the filtenna, which would provide a route for unwanted out-of-band signals to pass into the receiver. Further,

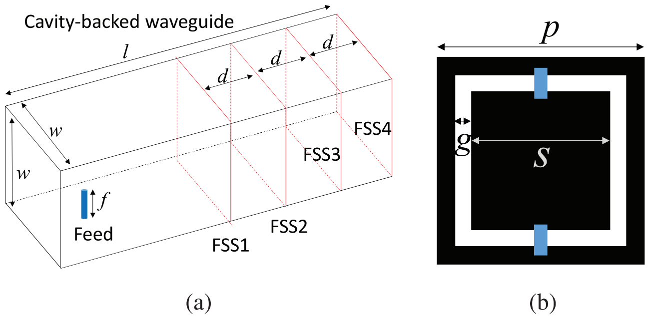

FIGURE 2 Reconfigurable filtenna: (a) Whole filtenna, (b) FSS unit cell. $l = 285$ mm, $d = 57$ mm, $w = 112.5$ mm, $f = 35$ mm, $p = 22.5$ mm, $g = 1$ mm, $s = 15$ mm

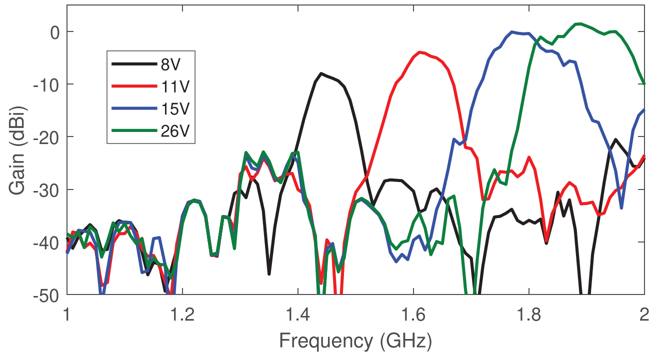

FIGURE 4 Filtenna gain against frequency at various bias voltages

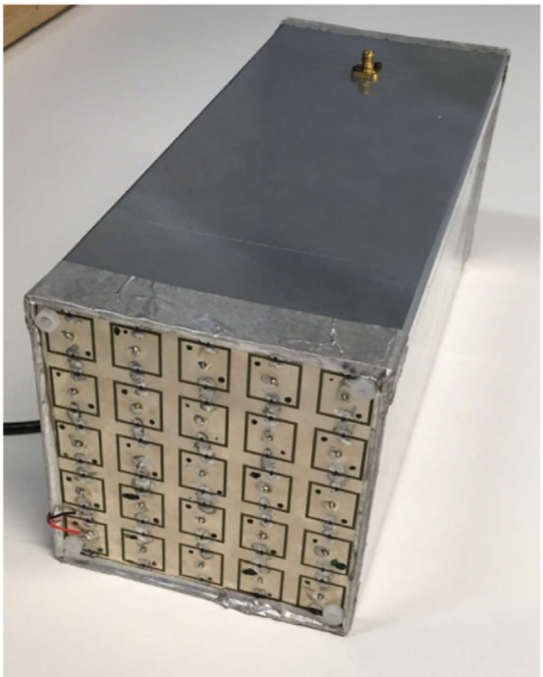

FIGURE 3 Photograph of the fabricated reconfigurable filtenna

the biasing wires and apertures in the filtenna's waveguide were covered with conducting aluminium tape to provide additional shielding to unwanted leakage of high frequency currents into and out of the filtenna.

To evaluate the filtenna's performance, its gain at boresight was measured against frequency in an anechoic chamber using an Agilent E5071C network analyzer, at a range of bias voltages (Figure 4). The filtenna is able to tune continuously from 1.94 GHz at 26 V, down to a gain 9 dB lower at 1.44 GHz with 8 V bias. The bandwidths increase from 55 to 160 MHz as the centre frequency increases. The absolute gains are low, starting at 1.4 dBi and moving down to −8 dBi. This is particularly due to losses in the varactor diodes, which increase as the centre frequency is reduced due to the capacitance of the diodes being higher, so the current through the diodes and so the I^2R losses increasing. This could be improved by using lower resistance diodes, as well as lower loss substrates. The filtenna's gain could also be increased by increasing the directivity of the filtenna through flaring the receiving end of the waveguide.

However, the OOB rejection is very promising, with most frequencies over the 1.4 to 2.0 GHz operating range experiencing over 30 dB rejection. At some frequencies, this does increase to at worst 12 dB rejection, most likely due to coupling into the filtenna through small apertures caused by manufacturing defects. As such, despite the low gain, the prototype was deemed sufficient to investigate the performance of reconfigurable filtennas in SDR receivers further.

To ensure rejection is maintained when interference is incident from all directions, the filtenna's radiation pattern was measured at 1.44 and 1.94 GHz with both 8 and 26 V bias voltages applied (Figure 5). At 8 V, the filtenna provides at least 14 dB rejection of the unwanted 1.94 GHz frequency across the whole E-plane (Figure 6a), and at least 16 dB rejection across the whole H-plane (Figure 6b). It also has a 90° beamwidth in the E-plane and 85° in the H-plane at 1.44 GHz. At 26 V, the desired 1.94 GHz signal beamwidths are 85° in the E-plane and 75° in the H-plane, suggesting some of the lower gain at 1.44 GHz is due to reduced directivity at the lower frequency. The patterns are asymmetric due to the biasing wires on one side of the E-plane and the feed on one side of the H-plane. The rejection at 26 V is good, with a minimum of 16 dB in the E-plane and 24 dB in the H-plane.

These rejection measurements should be analysed with care, as at very low received powers, such as those where the filtenna is detuned, measurement uncertainties become more pronounced. As such, while most unwanted signal presence will be due to leakage through bias wires and undesired apertures in the filtenna, some may be due to coupling in the measurement system itself. This means the results should be treated as a worst-case measurement of filter performance, and show that the filtenna is capable of providing good rejection at key frequencies across a wide range of angles of arrival.

The filtenna's intermodulation performance in the presence of strong signals was then measured. This is an important parameter as the varactor diodes become non-linear as the strength of incident signals increases, and high-powered blockers may cause intermodulation products to interfere with the desired signal. To maximise the power incident on the diodes, the performance is measured using the filtenna in transmit

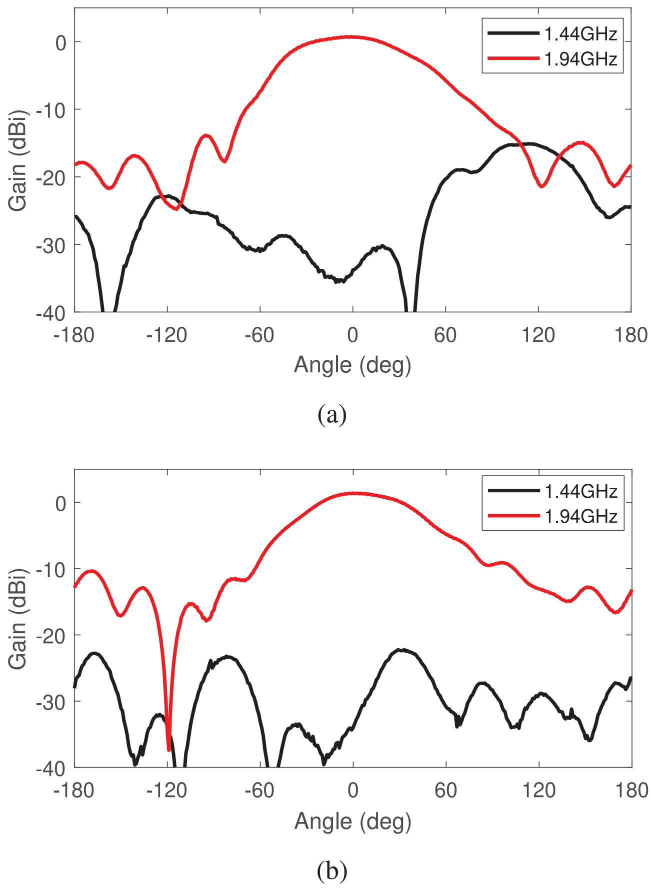

FIGURE 5 Filtenna radiation pattern at 26V bias: (a) E-plane cut, (b) H-plane cut

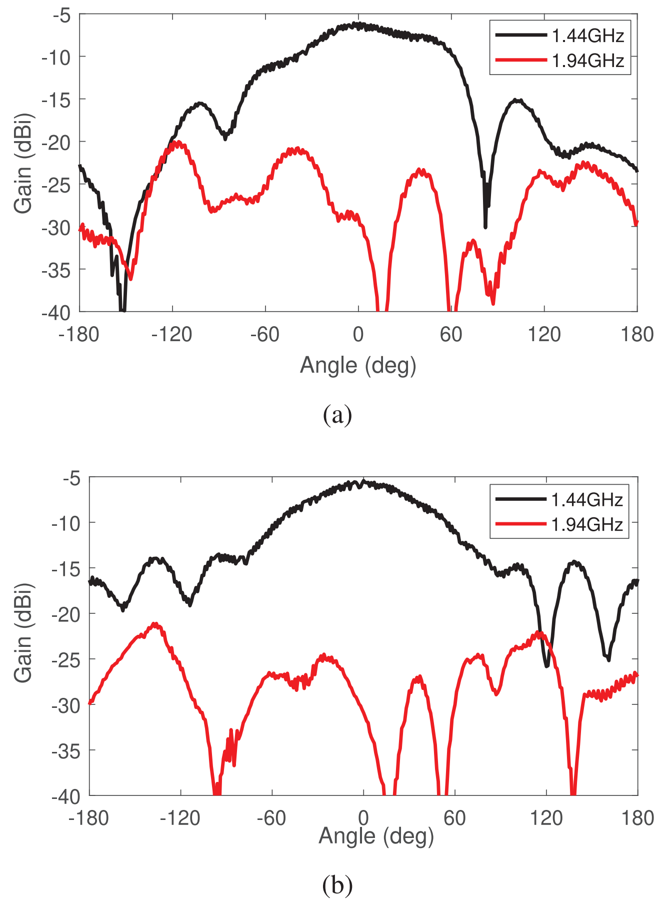

FIGURE 6 Filtenna radiation pattern at 8V bias: (a) E-plane cut, (b) H-plane cut

mode as shown in Figure 7. The filtenna is connected to a Keysight N5245B PNA-X microwave network analyzer, which inserts into it two tones of frequency f_1 and f_2 spaced Δf apart in frequency while maintaining a mean value of 1.8 GHz. It is placed at boresight 0.5 m from a passive horn antenna with gain 8 dBi at 1.8 GHz. The filtenna is biased at 18.5 V to make its centre frequency 1.8 GHz. It is assumed that the non-linearities of the filtenna are reciprocal in receive mode, with equivalent input power causing the same intermodulation products to be generated.

First, the two tones are transmitted at the maximum output power of the spectrum, 5 dBm, while Δf is varied. The power in the third order modulation products (IM_3) is measured, and shown in Figure 8a compared with the power of the received fundamental signals. The IM_3 appears 50 dB below the fundamentals when the intermodulation products appear within the bandwidth of the filtenna response. However, as Δf is increased such that the IM_3 products begin to fall outside the filter bandwidth, the power in the products start to reduce in power, eventually falling below the measurement noise floor. This suggests that the filtenna's non-linearity will most likely be a problem only for blockers that occur within the filter passband and produce intermodulation products in the passband region, while others will be filtered as expected by the filtenna.

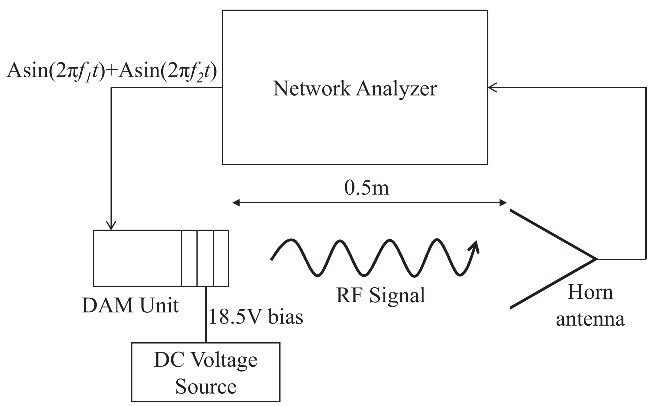

FIGURE 7 Experimental setup for measuring the non-linearities of the filtenna

Next, the 3rd order intercept point (IP3) of the filtenna is measured by setting $\Delta f = 10$ MHz and increasing the power of the transmitted signals, while measuring the power in the received fundamental and IM_3 products. The input power ranges from -5 dBm, where the IM_3 products appear above the noise floor, to the maximum transmit power 5 dBm. After this, the trend is extended to find an IP3 of 31 dBm, which is significantly higher than most LNAs in this band, which may

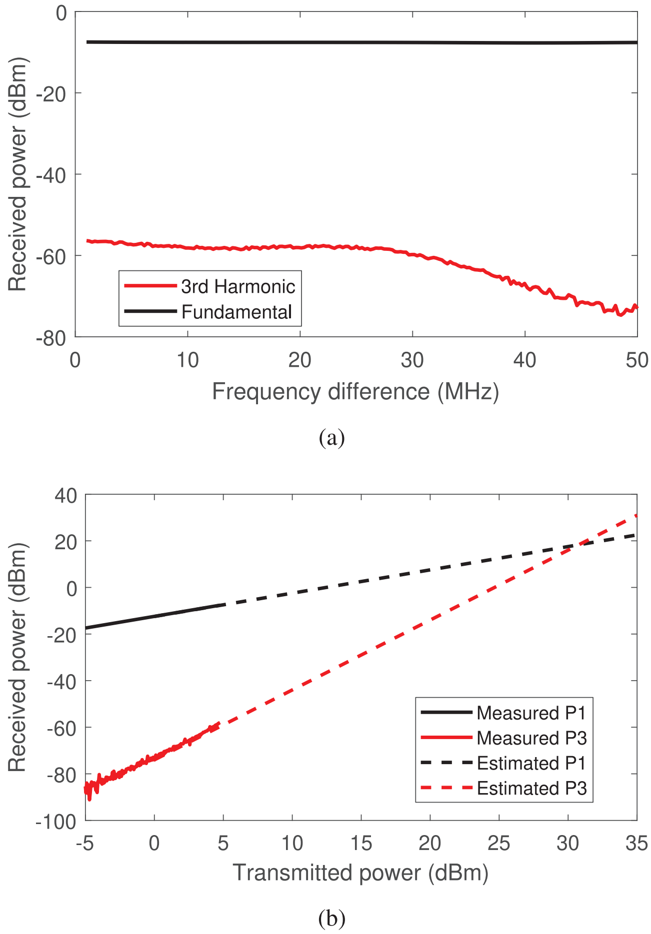

FIGURE 8 Intermodulation products in filtenna subject to two interference tones: (a) varying Δf while P_{in} = 5 dBm; (b) varying P_{in} while Δf = 10 MHz

TABLE 1 Filtenna and commercially available filter characteristics

	Filtenna	Analog ADMV8526 [17]	Netcom 5694-7 [18]
Tuning range (GHz)	1.45–1.95	1.25–2.60	1.25–1.85
Typical bandwidth (%)	9	9	7
20 dB Rejection low side (% f_{centre})	95	85	67
20 dB Rejection high side (% f_{centre})	106	116	110

have IP3s of around 17 dBm [16]. As such, while the filtenna's non-linearity may add some interference from intermodulation products, they are unlikely to be dominant in most receivers it is included in.

Finally, the filter characteristics of the filtenna are compared with commercially available bandpass filters in Table 1. The two commercial filters have a broader range of tuning than the filtenna, but similar bandwidths. The insertion loss of both filters ranges from 4 to 7 dB with tuning, though this is difficult to compare with the gain of the filtenna. However, the filter roll-off of the filtenna is much higher than the commercial filters due to it being a higher order filter, reaching 20 dB within 6% of the centre frequency rather than 15% or even 33% for the low side of the Netcom filter. In a system context, this means a receiver attempting to receive a 1.6 GHz signal with an unwanted signal at 1.7 GHz would achieve 20 dB rejection with the filtenna, but only 5dB rejection with the Analog filter and 3 dB with the Netcom filter. This suggests a strong advantage for using the proposed filtenna to mitigate adjacent band interference, especially in frequency division duplexing and carrier aggregation schemes.

4 | RECEIVER CHARACTERISATION

In order to evaluate the performance of the filtenna-based receiver, it was implemented in an OTA HWIL testbed (Figure 9). Long-term evolution (LTE) downlink signals were used in all tests [19], though the receiver could be adapted for most wireless standards. The receiver's RF front-end consists of the filtenna and a Mini-circuits ZX60-83LN12+ LNA, which provides 21dB gain across 0.5–8 GHz. Note that an LNA operating over only 1.4–2 GHz would be sufficient for the tests reported and would likely improve rejection of noise and signals outside the operating region of the receiver. The ADC is implemented using a LeCroy WaveMaster 813Zi-A oscilloscope, sampling at 5 GSample/s with 8 bits resolution and set to a 4-GHz RF bandwidth. In place of AGC amplification, the dynamic range of the ADC is varied manually to ensure the whole received RF signal is sampled. The digital back-end is implemented in LabVIEW operating on a NI PXIe-8135 chassis, using a DCO based DDC and a Chebyshev finite impulse response (FIR) LPF provides channel filtering. Baseband processing is performed in LabVIEW's LTE Application Framework (LTE-AF) [20], extracting the physical downlink shared channel to calculate an error vector magnitude (EVM) of the constellation, and decoding the physical downlink control channel (PDCCH) in order to calculate a block error rate (BLER). Format 1 of the PDCCH was used as described in LTE Release 10, carrying 144 bits in QPSK modulation [19]. EVM values were only measured when successful synchronisation was achieved.

The transmitter also used the PXIe chassis, with the wanted LTE signal generated by the LTE-AF with a NI-5793 FlexRIO RF Adapter Module, and the interferer generated in LabVIEW and transmitted from an NI-5793 transmitting RF Adapter Module. The lower-frequency signal is amplified by a Pasternack PE15A4019 wideband power amplifier (PA), and the higher signal is amplified by a HP 8349B PA. These are then filtered by Minicircuits VBFZ-1400-S+ or VBFZ-2130-S+ filters for the low and high bands, respectively, to minimise interference due to PA non-linearities. Finally the signals are combined and transmitted through a wideband horn antenna in an anechoic chamber (Figure 10).

Although the receiver is continuously tunable, it was tested at centre frequencies 1.44 and 1.94 GHz with the filtenna biased at 8 and 26 V, respectively, in order to characterise performance

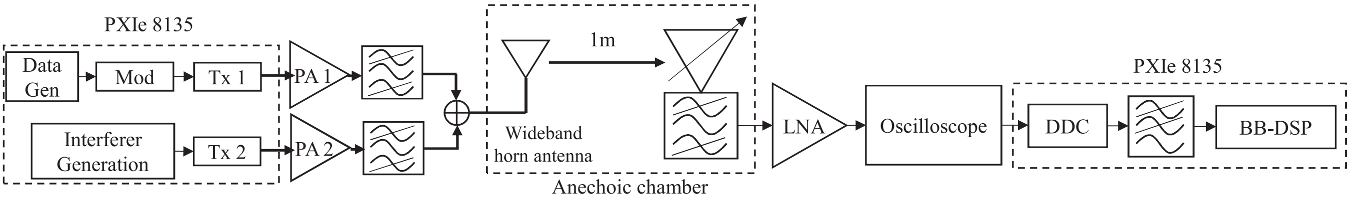

FIGURE 9 Experimental testbed for evaluating tunable filtenna-enabled direct RF sampling receiver

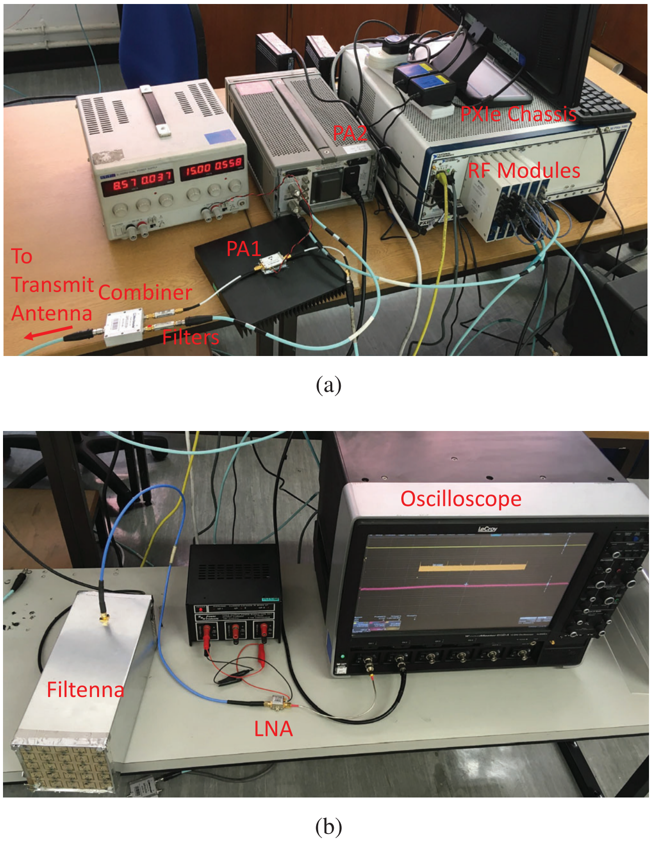

FIGURE 10 Photograph of testbed setup: (a) transmitter setup; (b) receiver setup

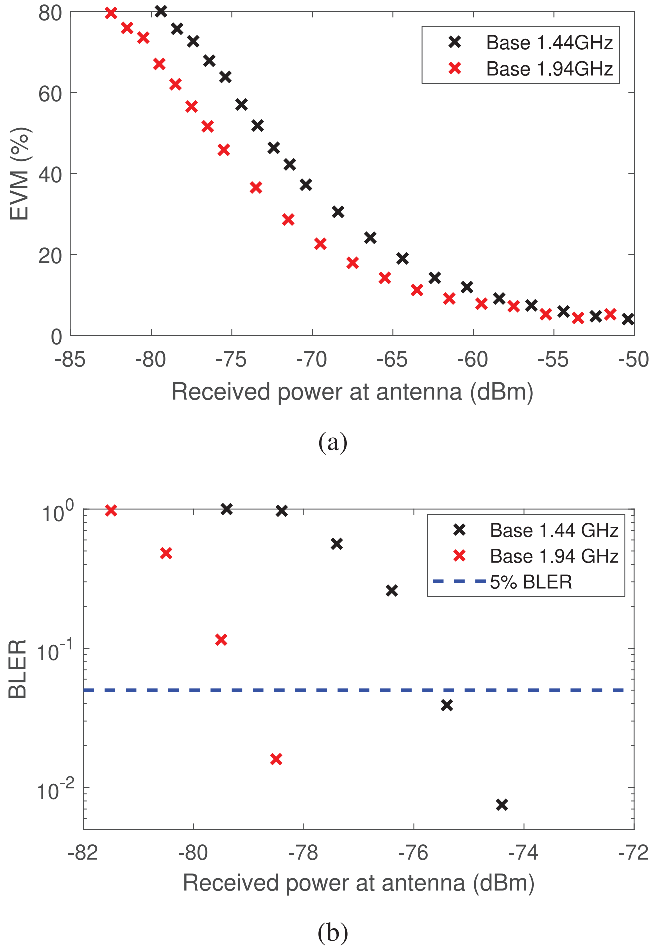

FIGURE 11 (a) EVM and (b) BLER baseline measurements of filtenna-based receiver architecture operating at 1.44 and 1.94 GHz

at the extreme available frequencies. Three tests were carried out. First, a baseline measurement with a 20 MHz LTE signal with QPSK modulation transmitted from TX1 was performed, with PA2 switched off. The transmitted power was varied and both EVM and BLER were measured. The results are shown in Figure 11 against the received power at the antenna.

Both EVM measurements exhibit approximately a classic $1/\mathrm{SNR}^2$ shape, though at low received powers the measured values are slightly below this trend due to a bias toward signals which achieve synchronisation with the receiver, and at high received powers, there is a floor at approximately 4%, likely due to a mix of both hardware impairments and the digital quantisation noise introduced by the oscilloscope, which increases with the desired signal power (Figure 11a). There is a difference of 3 dB between the 1.44 GHz and the 1.94 GHz signal, mostly due to the higher gain of the filtenna at higher frequencies. The BLER, meanwhile, falls in the typical waterfall style, reaching the 5% error rate at −79 dBm for the 1.94 GHz measurement and −75.5 dBm for the 1.44 GHz measurement, which maintains the approximately 3 dB difference seen in the EVM measurements. 5% is used as the acceptable performance point, as here the receiver achieves 95% of its throughput for a given modulation scheme.

Second, an OOB blocking test was carried out, following the requirements for OTA testing in 5G NR [21]. This involved a continuous wave (CW) signal at a blocking frequency illuminating the antenna at boresight with electric field strength 0.36 V/m, and measuring any degradation in EVM and BLER. The OTA standard allows up to 6 dB degradation in

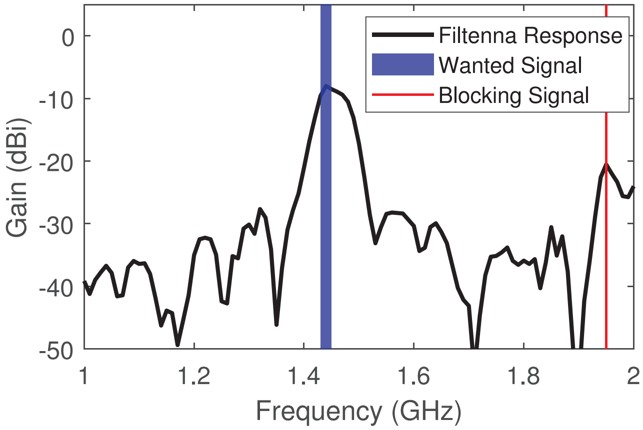

(a)

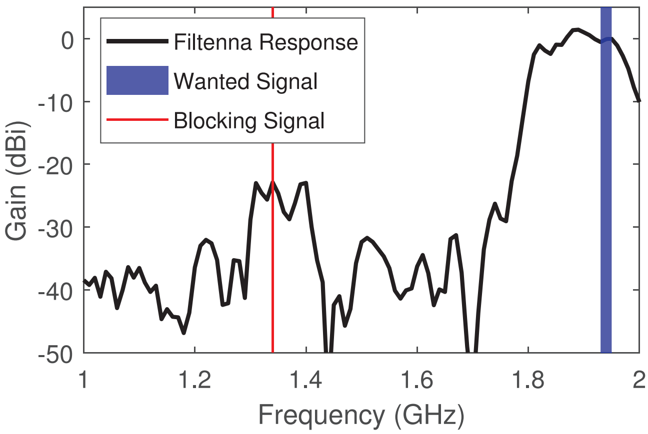

(b)

FIGURE 12 Gain response of the filtenna with highlighted regions representing the wanted LTE signal and unwanted OOB blocker in frequency, setup for (a) 1.44 GHz operation with bias voltage 8 V; (b) 1.94 GHz operation with bias voltage 26 V

performance from the presence of such OOB blockers. The 5G NR Standard requires good operation across all incident frequencies between 30 MHz and 12.75 GHz, but for simplicity only key frequencies were tested. In particular, it was assumed that the worst-case blocker for the receiver is at the highest out-of-band gain of the filtenna. When the filtenna is biased at 8 V for operation at 1.44 GHz, this point is 1.95 GHz, where a gain of −21 dBm was measured (Figure 12a), while when the filtenna was biased at 26 V for reception of signals at 1.94 GHz, highest OOB gain is −23 dBm at 1.34 GHz.

The CW interferer was set as shown in Figure 12 with a fixed power, while the wanted signal's transmit power is varied. Even with the worst-case blockers, the combination of the filtenna's band filtering and FIR filter's channel filtering means no degradation in performance was observed, with identical EVM and BLER performance to that seen in Figure 11. This is partly due to the filtenna performance, which reduces the incident blocker to a received power at the LNA input of −53 dBm when operating at 1.44 GHz, and −52 dBm when operating at

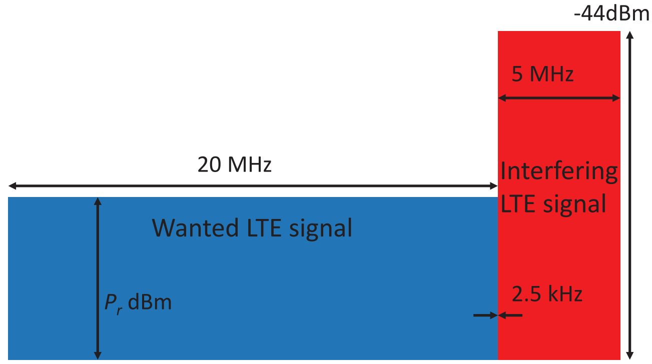

FIGURE 13 Frequency and power distribution of wanted and interfering signals for the ACS performance test

1.94 GHz, ignoring cable losses which would reduce this further. These are still not insignificant signal powers, but they are low enough to avoid any distortion from the LNA or significant loss of sensitivity in the ADC, even at low wanted signal powers. The digitised signal is suppressed well by the lowpass filtering after the DDC, allowing good operation even in the presence of the blocker, suggesting this receiver is suitably resilient to OOB blocking.

The third and final test is of ACS performance, again using the 5G NR OTA standard tests [21]. A 5 MHz QPSK modulated LTE interfering signal is generated with 2.5 kHz gap between the edge of its signal and the 20 MHz desired signal (Figure 13). The interferer is set so the average received power at the input to the receiver's LNA is −44 dBm, chosen as this is the required test power in the standard for a close-area base station. Note that this means any effect of the filtenna is ignored, as it is assumed that the close interfering signals are within the passband of the filtenna. The desired signal power P_r is varied around the noise floor, and the received EVM and BLER are measured. As with the baseline and OOB blocking tests, the receiver is measured with QPSK-modulated desired signals centred first at 1.44 GHz, and then at 1.94 GHz, to evaluate performance at the extremes of the receiver's operation region.

The combined results for this and the first test are shown in Figure 14 when operating at 1.44 GHz, and Figure 15 when the receiver is operating at 1.94 GHz. The baseline measurements are included for ease of comparison. A 5G NR standard-compliant close-area base station receiver should operate with less than 6 dB degradation in the presence of the wideband in-band blocker. In comparison, taking measurements of the EVM at the required operating point for QPSK modulated signals of 17.5%, there is approximately 2 dB degradation in EVM performance at 1.44 GHz (Figure 14a), and similarly 2 dB degradation at 1.94 GHz (Figure 15a). Meanwhile, in BLER performance, for the required 5% error rate, the required receive power at the antenna increases from −75.5 to −74.5 dBm at 1.44 GHz in the presence of blockers, while at 1.94 GHz, it increases from −79 to −76 dBm, a 3 dB degradation.

It should be noted that the ACS measurement is largely a measure of digital channel filter performance. The single filter used here has 398 taps, which in some applications

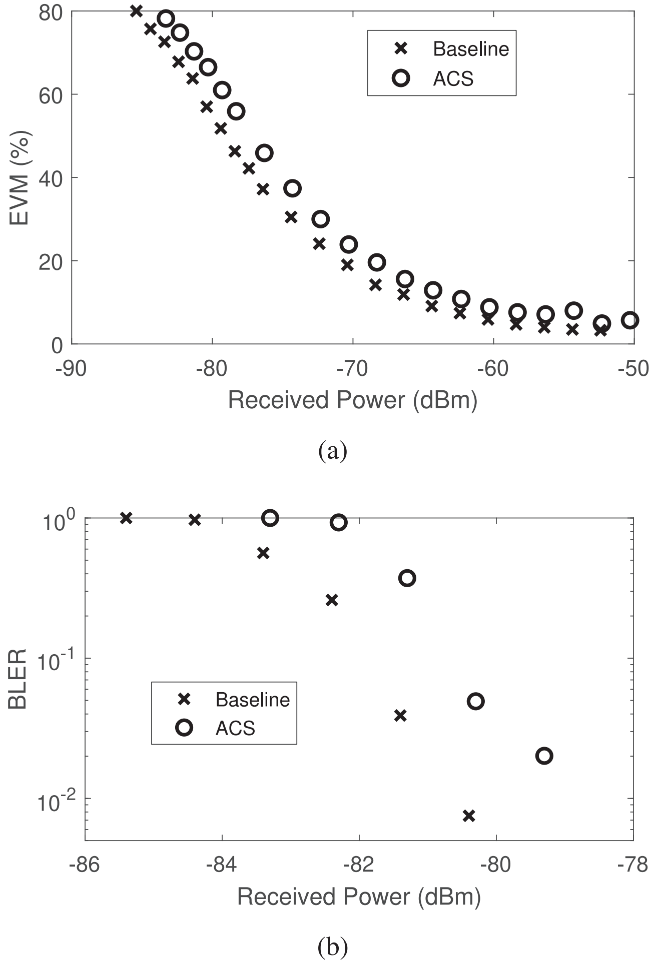

FIGURE 14 (a) EVM and (b) BLER measurements of filtenna-based receiver operating at 1.44 GHz, with and without a close-area BS blocker

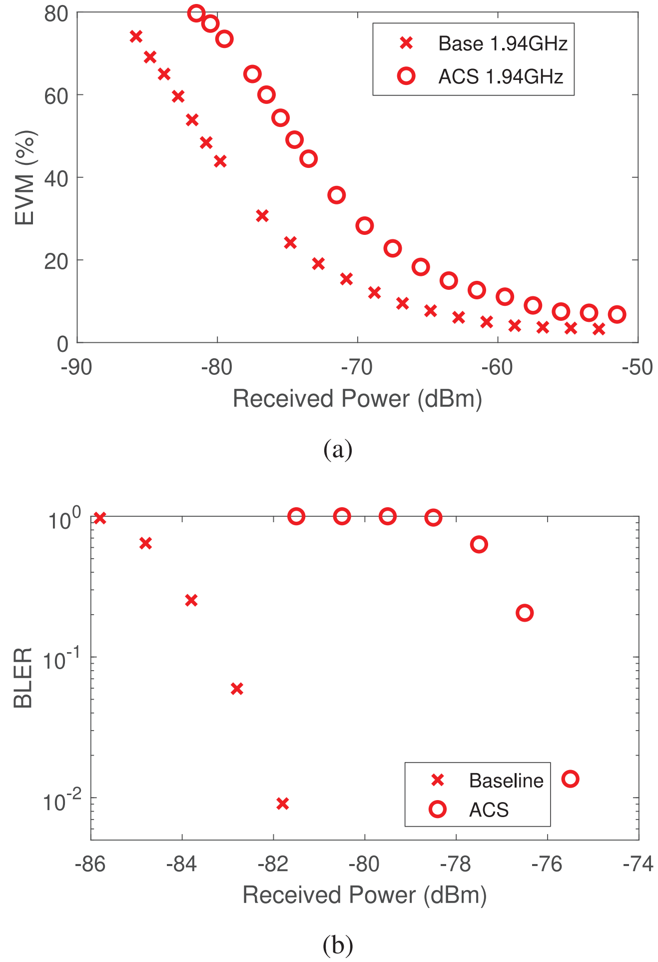

FIGURE 15 (a) EVM and (b) BLER measurements of filtenna-based receiver operating at 1.94 GHz, with and without a close-area BS blocker

could use too much resource in a SDR. However, this can be reduced by using multi-stage DDC filters such as cascaded integrator-comb decimators. This is left to future work, as the proof-of-concept here shows that a reconfigurable filtenna-based tunable direct RF sampling receiver could achieve OTA standard compliant performance.

5 | CONCLUSIONS

A tunable direct RF sampling receiver, enabled by a reconfigurable FSS-based filtenna, has been proposed and demonstrated. The receiver architecture was introduced with a reconfigurable filtenna, for band filtering, and a wideband LNA comprising the RF front-end followed by a Nyquist sampling ADC and software downconversion, channel filtering and baseband processing. The filtenna was characterised in detail in both frequency and angle, showing at worst 12 dB rejection. The intermodulation performance was also explored, with a measured IP3 of 31 dBm suggesting that non-linear effects would be dominated by the LNA performance. Finally, the receiver was implemented in a HWIL OTA testbed using LTE signals, and the EVM and BLER were measured. When subject to OOB blocking tests, the combination of the filtenna and digital processing meant the blockers produced no degradation in performance, while in ACS tests at most 3 dB degradation in BLER was measured, which is within the 5G NR specification. Future work will explore using reconfigurable filtennas with tunable direct RF subband sampling architectures, and implement lower complexity DDC architectures.

AUTHOR CONTRIBUTIONS

Stephen Henthorn: Conceptualization, investigation, software, writing - original draft. Kenneth Lee Ford: Supervision, writing - review and editing. Timothy O'Farrell: Conceptualization, funding acquisition, supervision, writing - review and editing.

ACKNOWLEDGEMENT

This work was financially supported by the United Kingdom's "Engineering and Physical Sciences Research Council" (EPSRC) on grant numbers EP/M013723/1 and EP/S008101/1.

CONFLICT OF INTEREST

The authors have declared no conflict of interest.

DATA AVAILABILITY STATEMENT

Data is available at https://doi.org/10.15131/shef.data.20804953.v1.

ORCID

Stephen Henthorn https://orcid.org/0000-0003-1913-9283

REFERENCES

1. Mitola, J.: The software radio architecture. IEEE Commun. Mag. 33(5), 26–38 (1995)
2. Bahramzy, P., Olesen, P., Madsen, P., Bojer, J., Caporal Del Barrio, S., Tatomirescu, A., et al.: A tunable RF front-end with narrowband antennas for mobile devices. IEEE Trans. Microwave Theory Tech. 63(10), 3300–3310 (2015)
3. Henthorn, S., O'Farrell, T., Asif, S.M., Anbiyaei, M.R., Ford, K.L.: Tri-band single chain radio receiver for concurrent radio. In: 2020 2nd 6G Wireless Summit (6G SUMMIT), pp. 1–5. IEEE, Piscataway, NJ (2020)
4. Henthorn, S., Mohammadkhani, R., O'Farrell, T., Ford, K.L.: The effect of ADC resolution on concurrent, multiband, direct rf sampling receivers. In: 2021 IEEE Global Communications Conference (GLOBECOM), pp. 1–6. IEEE, Piscataway, NJ (2021)
5. Luo, G.Q., Hong, W., Tang, H.J., Chen, J.X., Yin, X.X., Kuai, Z.Q., et al.: Filtenna consisting of horn antenna and substrate integrated waveguide cavity FSS. IEEE Trans. Antennas Propag. 55(1), 92–98 (2007)
6. Li, W.T., Hei, Y.Q., Subbaraman, H., Shi, X.W., Chen, R.T.: Novel printed filtenna with dual notches and good out-of-band characteristics for UWB-MIMO applications. IEEE Microwave Wireless Compon. Lett. 26(10), 765–767 (2016)
7. Tawk, Y., Costantine, J., Christodoulou, C.G.: Reconfigurable filtennas and MIMO in cognitive radio applications. IEEE Trans. Antennas Propag. 62(3), 1074–1083 (2014)
8. Fakharian, M.M., Rezaei, P., Orouji, A.A., Soltanpur, M.: A wideband and reconfigurable filtering slot antenna. IEEE Antennas Wirel. Propag. Lett. 15, 1610–1613 (2016)
9. Tawk, Y., Costantine, J., Christodoulou, C.G.: A varactor-based reconfigurable filtenna. IEEE Antennas Wirel. Propag. Lett. 11, 716–719 (2012)
10. Tang, M.C., Wen, Z., Wang, H., Li, M., Ziolkowski, R.W.: Compact, frequency-reconfigurable filtenna with sharply defined wideband and continuously tunable narrowband states. IEEE Trans. Antennas Propag. 65(10), 5026–5034 (2017)
11. Kumar, A., Pathak, N.P.: Wireless monitoring of volatile organic compounds/water vapor/gas pressure/temperature using RF transceiver. IEEE Trans. Instrum. Meas. 67(9), 2223–2234 (2018)
12. Kantemur, A., Tak, J., Siyari, P., Abdelrahman, A.H., Krunz, M., Xin, H.: A novel compact reconfigurable broadband antenna for cognitive radio applications. IEEE Trans. Antennas Propag. 68(9), 6538–6547 (2020)
13. Henthorn, S., Ford, K.L., O'Farrell, T.: Direct antenna modulation for high-order phase shift keying. IEEE Trans. Antennas Propag. 68(1), 111–120 (2020)
14. Kasar, O., Belen, M.A.: Realization of reconfigurable filtering horn antennas using active frequency selective surfaces for GSM and LTE signal filtering. Int. J. RF Microwave Computer-Aided Eng 30(11), 422–429 (2020). https://onlinelibrary.wiley.com/doi/abs/10.1002/mmce.22429
15. Barrak, R., Othman, A., Abib, G.I., Muller, M., Mabrouk, M., Ghazel, A.: Design of a tunable anti-aliasing filter for multistandard RF subsampling GNSS receivers. IEEE Trans. Circuits Syst. II Express Briefs 66(2), 207–211 (2019)
16. Infineon.: Silicon germanium low noise amplifier: BGA824N6 application note. Infineon, (2014). BGA824N6. rev. 1.0. https://www.infineon.com/dgdl/Infineon-AN403-AN-v01_00-EN.pdf?fileId=5546d4624b0b249c014b1746f4d55aac
17. Analogue Devices.: ADMV8526 1.25 GHz to 2.60 GHz Digitally Tunable Band-Pass Filter. Analogue Devices, (2021). Rev 0. https://www.analog.com/media/en/technical-documentation/data-sheets/admv8526.pdf
18. Netcom RF & Microwave Technology.: Model 5694-7 - Tunable Filter 1.25-1.85GHz. Netcom RF & Microwave Technology, (2021). Rev 3. https://www.netcominc.com/wp-content/uploads/2022/05/444411290-website-model-5694-7-1.25-1.85ghz-tunable-filter-cutsheet-_-netcom_-inc._-02122021.pdf
19. 3GPP.: Evolved Universal Terrestrial Radio Access (E-UTRA); Physical Channels and Modulation (3GPP TS 36.211 version 10.7.0 Release 10). 3GPP, 2013
20. National Instruments.: LabVIEW Communications LTE Application Framework 2.0 and 2.0.1. National Instruments, Updated (2020). https://www.ni.com/en-gb/support/documentation/supplemental/16/labview-communications-lte-application-framework-2-0-and-2-0-1.html
21. 3GPP.: NR; Base Station (BS) conformance testing; Part 2: Radiated conformance testing (3GPP TS 38.141-2 version 16.4.0 Release 16). 3GPP, 2020

How to cite this article: Henthorn, S., Ford, K.L., O'Farrell, T.: A system-level performance evaluation of a reconfigurable filtenna in the presence of in- and out-of-band blockers. IET Commun. 1–9 (2022). https://doi.org/10.1049/cmu2.12504